IEICE Proceeding Series

Radio-over-Fiber Applications of Semiconductor Lasers in Period-One Oscillation

Jun-Ping Zhuang, Xiao-Zhou Li, Song-Sui Li, Sheng-Kwang Hwang, Sze-Chun Chan

Vol. 1 pp. 466-469
Publication Date: 2014/03/17
Online ISSN: 2188-5079

2012 International Symposium on Nonlinear Theory and its Applications
NOLTA2012, Palma, Majorca, Spain, October 22-26, 2012

Radio-over-Fiber Applications of Semiconductor Lasers in Period-One Oscillation

Jun-Ping Zhuang[1], Xiao-Zhou Li[1], Song-Sui Li[1], Sheng-Kwang Hwang[2,3], and Sze-Chun Chan[1,*]

[1]Department of Electronic Engineering, City University of Hong Kong, Hong Kong, China
[2]Department of Photonics, National Cheng Kung University, Taiwan
[3]Advanced Optoelectronic Technology Center, National Cheng Kung University, Taiwan
*Email: scchan@cityu.edu.hk

Abstract– The period-one (P1) nonlinear dynamics of an optically injected single-mode semiconductor laser is considered for radio-over-fiber (RoF) communication. By introducing double locking from both optical and microwave injections, the laser acts to convert uplink microwave signals to upstream optical signals. In particular, communication at 24 GHz, which is beyond the conventional limit of relaxation resonance, is thoroughly investigated. Tailoring optical spectra of the P1 oscillations successfully suppresses the effects of chromatic dispersion of RoF transmission.

1. Introduction

Nonlinear dynamics of semiconductor lasers continue to attract researchers due to the profound potential in high-speed photonic applications. Interesting dynamics including four-wave mixing, stable locking, periodic oscillation, and chaotic oscillation have been investigated for applications such as random bit generation [1], chaotic ranging [2-3], secure communication [4-6], signal conversion [7-9], and tunable microwave generation [10-11]. Recently, the period-one (P1) oscillations of optically injected lasers have been experimentally demonstrated for radio-over-fiber (RoF) applications [12]. Owing to the induced instability in the coupling between the population inversion and the intra-cavity optical field, the modulation bandwidth of an injected laser can be greatly enhanced when operating in P1 oscillation, so wireless microwave signals can be easily injected into the laser for transmission over optical fibers. For instance, with a 2.5-Gbps-grade single-mode laser, RoF uplink transmission at 16 GHz was realized with a low bit error rate (BER). The approach has the advantage of employing no expensive microwave electronics because the inherently fast P1 oscillation was responsible for the subcarrier generation [12]. A wide tuning range was also enabled by manipulating the injection parameters because of the tunable red-shift effect of the injected cavity [13]. Low BER can be maintained by optimizing the optical spectrum of the P1 oscillation in mitigating the effects of chromatic dispersion [14].

RoF communication with subcarrier frequencies at tens of gigahertz has been of significant technological importance due to the ever-increasing demand on data rate [15]. RoF uses optical carriers modulated with microwave subcarriers for optical transmission through optical fibers between the central office and remote base stations. Benefits of employing RoF include the centralization of expensive microwave electronics, low loss, immunity to radio frequency interference, high cell density, and large bandwidth [12,15].

In this work, the P1 dynamics of an optically injected single-mode semiconductor laser is investigated for uplink RoF communication. The laser is subject to both optical and microwave injection-locking so that the uplink microwave signal is converted to an upstream optical signal. Following this introduction, the model for the numerical study is presented, which is followed by the results on the locking quality, the effect of optical filtering on all-optical demodulation, and the effect of fiber dispersion on electrical demodulation. Finally, the last section gives a summary.

2. Setup and Model

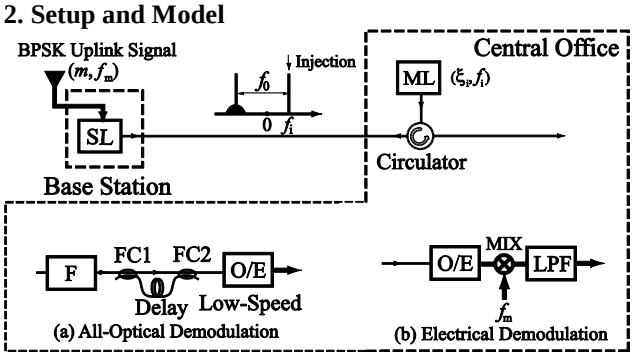

Fig. 1. Schematic of employing an optically injected laser for the RoF uplink with (a) all-optical or (b) electrical demodulation. SL: slave laser. ML: master laser. LPF: low pass filter. F: optical bandpass filter. MIX: microwave mixer. FC: 3-dB fiber coupler. Thin and thick lines correspond to optical and microwave paths, respectively.

The RoF uplink setup is illustrated in Fig. 1. A master laser at the central office optically injects the slave laser at the base station through an optical circulator. The downstream injection of the master laser is detuned at frequency f_i above the free-running frequency of the slave laser. The injection strength ξ_i, defined as the normalized field strength injected into the slave laser, can be controlled by controlling the master laser. The slave laser

is optically injection-locked by the master laser and regenerates the injected optical frequency. Moreover, by selecting the injection parameters (ξ_i, f_i) properly, the relaxation resonance of the slave laser is undamped into P1 oscillation at a microwave frequency f_0. Then, an uplink signal at subcarrier frequency f_m is applied as a current modulation into the slave laser with a current modulation index m, which is normalized to the bias current above threshold. The frequency f_0 is adjusted by varying (ξ_i, f_i) so that the P1 oscillation can be further locked by the subcarrier frequency f_m. Such double-locking effectively converts the uplink microwave data into upstream optical data when binary phase-shift keying (BPSK) is adopted [12,14].

Two schemes are employed for demodulation in the central office. Figure 1(b) presents an electrical demodulation scheme. The optical signal that carries the BPSK data is electronically mixed, after optoelectronic conversion, with a local oscillator at f_m. The signal is then low-pass filtered to obtain the demodulated signal. Figure 1(a) presents an all-optical demodulation scheme using a delayed-homodyne technique. As an option, the optical signal can first be filtered by an optical bandpass filter so as to select only one or all of the optical frequency components for subsequent demodulation. Then the signal is sent to an optical fiber delay-line interferometer, where consecutive bits are interfered optically. Lastly, data can be recovered by simply using a low-speed optical-to-electrical converter (O/E) at the baseband. The quality of the demodulated signal is then quantified by estimating the quality Q of the corresponding eye-diagram.

The slave laser is a single-mode semiconductor laser modeled by the Class B laser rate equations [16]. The dynamics of the slave laser are described by the normalized intracavity optical field amplitude and the normalized charge-carrier density that are governed by the rate equations with a modulation term on the bias current [16]. The following laser dynamical parameters extracted from experiments are adopted throughout the simulations [16]: cavity decay rate $\gamma_c = 5.36\times10^{11}$ s^{-1}, spontaneous carrier relaxation rate $\gamma_s = 5.96\times10^{9}$ s^{-1}, differential carrier relaxation rate $\gamma_n = 7.53\times10^{9}$ s^{-1}, nonlinear carrier relaxation rate $\gamma_p = 1.91\times10^{10}$ s^{-1}, linewidth enhancement factor $b = 3.2$, and the normalized bias current above threshold $\tilde{J} = 1.222$. From these parameters, the relaxation resonance frequency is given as 10.25 GHz [13,17]. Second-order Runge-Kutta integration is then conducted.

3. Double Locking

Even with optical injection only, the P1 oscillation at f_0 can be generated. However, due to intrinsic spontaneous emission noise, the P1 oscillation is always associated with non-zero phase variance as noise. Modulation at frequency f_m applied at the bias current is thus needed to further lock the P1 oscillation. The quality of such double locking is quantified by the P1 oscillation phase noise variance, which is plotted in Fig. 2 as a function of frequency difference $f_m - f_0$. The phase noise is minimized when the frequency difference is small. The range of frequency difference with small phase variance below 0.1 rad^2 is referred to as the locking range [14]. Figure 2 verifies that the locking range increases with the modulation index m. The phase variance is estimated by integrating the normalized single sidebands between 3 MHz and 10 GHz away from f_m.

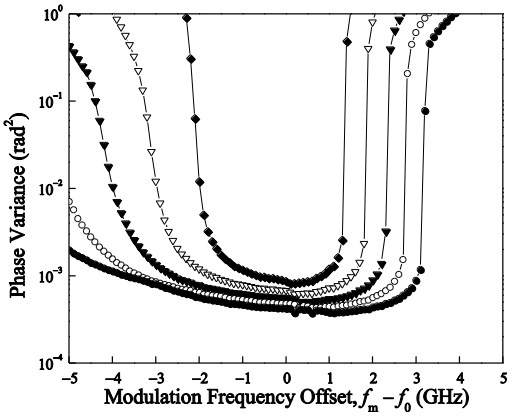

Fig. 2. Phase variance of the P1 oscillation at f_0 = 24 GHz subject to locking of current modulation at frequency f_m when the modulation index m = 0.10 (closed diamonds), 0.20 (open triangles), 0.30 (closed triangles), 0.40 (open circles), and 0.50 (closed circles). The slave laser is under injection of (ξ_i, f_i) = (0.18, 12.7 GHz).

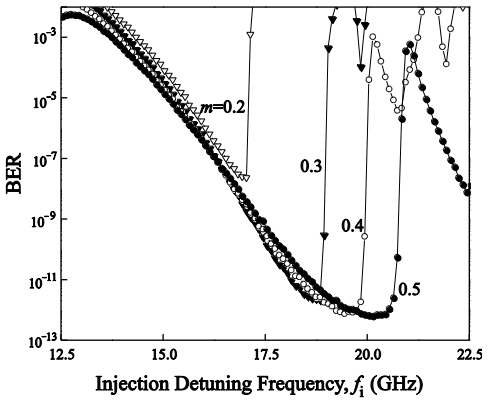

Fig. 3. BER versus the injection detuning frequency f_i for different values of modulation index m as labeled. Injection strength is kept constant at ξ_i = 0.18. The uplink signal is at f_m = 24 GHz with data rate of 622 Mbps.

Moreover, when the current modulation carries BPSK data, the emission from the slave laser is forced to carry the same data optically. The all-optical demodulation in Fig. 1 is then considered. The resultant BER is shown in Fig. 3. It is observed that minimum BER occurs when f_i is fine-tuned so that f_0 is optimized in relation to f_m. Also, the minimum BER reduces as the modulation index m increases. This is consistent with the fact the locking range increases with m in double locking.

4. All-Optical Demodulation

When the all-optical demodulation scheme in Fig. 1(a) is adopted, there are contributions to the recover data from the regenerative component and the generated P1 component of the P1 optical spectrum. The two components are detuned from the free-running frequency of the slave laser by f_i and $f_i - f_m$, respectively [14]. The optical bandpass filter in Fig. 1 can be adopted to select just one or both the components of the optical spectrum for demodulation. The time series and the power spectra of the recovered data with both optical components, with the regenerative component only, and with the P1 component only are shown as Figs. 4(a), (b), and (c), respectively. Optical phase demodulations using the interferometer of Fig. 1(a) result in signals shown in dark, whilst amplitude demodulations without the interferometer result in signals shown in gray. Comparing the gray and dark lines in the first row, it is obvious that the amplitude signals are much weaker than the phase signals. Data cannot be demodulated correctly no matter which component is selected. The corresponding baseband power spectra in the second row indicate that the amplitude signal is at least 35 dB weaker than the phase signal. Additionally, observation from Figs. 4(b) and (c) reveals that data cannot be recovered correctly when the regenerative component is selected. On the other hand, when only the P1 component is selected, the time series of the recovered data shows correct demodulation in Fig. 4(c). The baseband power spectra in Figs. 4(b) and (c) reveal that the power levels of the recovered signals differ by more than 20 dB. Therefore, the optical BPSK data is mainly carried by the P1 component.

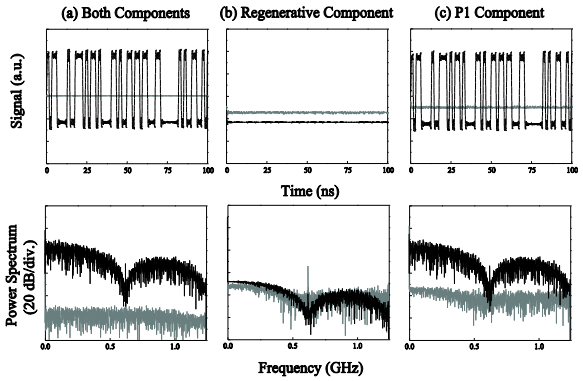

Fig. 4. Time series (first row) and the corresponding power spectra (second row) of the demodulated signal with different optical frequency component(s) selected by the optical bandpass filter. The dark lines are the demodulated phase signals obtained through the delayed-homodyne technique. The gray lines are the demodulated amplitude signals obtained through direct detection. (a) Both regenerative and P1 components included. (b) Only regenerative component included. (c) Only P1 component included.

5. Electrical Demodulation

For the electrical demodulation scheme in Fig. 1(b), beating of the optical frequency components from the slave laser is responsible for generating the microwave signal for subsequent down-conversion by the electrical mixer. The combined contribution from all optical frequency components of P1 oscillation affects the demodulation performance. Figure 5 shows the optical spectrum of the slave laser emitting in P1 oscillation consists mainly of the regenerative component at f_i, the P1 component at $f_i - f_m$, and another component at $f_i - 2f_m$ [13,17]. The frequencies are measured offset to the free-running frequency. The power ratio R of the weaker of the first two components over the last component is dependent on the injection parameters. For example, in Fig. 5(a), $(\xi_i, f_i) = (0.18, 20.1\ \text{GHz})$ so that the laser emits a nearly single sideband (SSB) spectrum with $R = 22.1$ dB. By contrast, in Fig 5(b), $(\xi_i, f_i) = (0.01, 23.6\ \text{GHz})$ so that laser emits a nearly double sideband (DSB) spectrum with $R = 1.3$ dB.

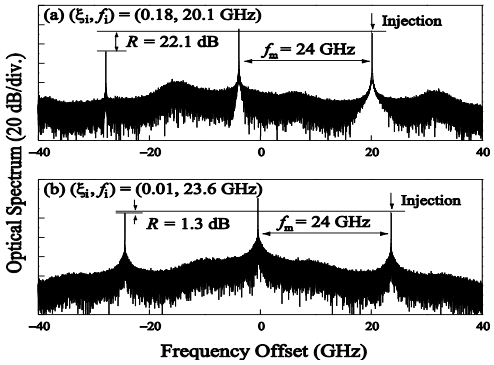

Fig. 5. Optical spectrum from the slave laser under current modulation of $(m, f_m) = (0.5, 24\ \text{GHz})$ without data. The optical injection parameters are adjusted to give (a) a nearly SSB spectrum and (b) a nearly DSB spectrum. The frequency axis is offset to the free-running frequency of the slave laser.

For P1 oscillation without data modulation, it has been investigated that SSB P1 oscillation is better than DSB P1 oscillation in terms of the immunity to chromatic dispersion-induced microwave power penalty [17]. When the P1 is double-locked with BPSK data, dispersion can cause power penalty as well as distortion of signals. A 622-Mbps BPSK uplink signal at $f_m = 24$ GHz is applied with modulation index $m = 0.5$ to modulate the slave laser under P1 oscillation with SSB and DSB, as in Figs. 5(a) and (b), respectively. Since the power spectra of P1 oscillations dictate the performances of electrical demodulation, they are shown in Fig. 6 by considering dispersion due to a standard Corning SMF-28 fiber at 1.55 μm. For the SSB P1 oscillation, the power spectra before and after transmission over a fiber length $l = 4.6$ km are presented in Figs. 6(a) and (b), respectively. There is no significant distortion or reduction of microwave power because the SSB optical spectrum. The fiber length is already the worse choice in terms of power penalty [17]. For comparison, the DSB P1 oscillation gives power spectra before and after transmission over $l = 1.6$ km in Figs. 6(c) and (d), respectively. The fiber length gives maximal power penalty for the DSB optical spectrum. Significant distortion of the power spectrum is clearly observed in Fig. 6(d). Therefore, it is important to

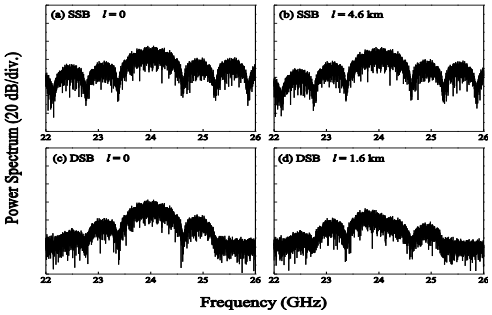

Fig. 6. Power spectra from the slave laser under uplink signal at f_m = 24 GHz. The system is in (a) SSB P1 oscillation with l = 0, (b) SSB P1 oscillation with l = 4.6 km, (c) DSB P1 oscillation with l = 0, and (d) DSB P1 oscillation with l = 1.6 km. The fiber lengths l in (b) and (d) are chosen at the first minima of microwave power for SSB and DSB, respectively.

operate the slave laser in SSB P1 oscillation by adjusting the injection parameters, which is consistent with power penalty minimization in photonic microwave transmission [14].

6. Conclusion

The P1 nonlinear dynamics of an optically injected laser offer interesting options for RoF uplink transmission. Optical injection first generates P1 oscillation at frequencies exceeding the laser bandwidth limited by the relaxation resonance, while a microwave modulation further locks the P1 oscillation. Such double locking imposes data onto the emission of the slave laser, where the P1 component of the optical spectrum is mainly responsible for carrying the data. All-optical demodulation is possible and requires no high-speed electronics. Electrical demodulation is also possible, but optimization of the optical spectrum to SSB is needed.

Acknowledgments

S. C. Chan's work was fully supported by a grant from the City University of Hong Kong under Project 7002674. S.K. Hwang's work was supported by the National Science Council of Taiwan under Contract NSC99-2112-M-006-013-MY3.

References

[1] A. Uchida, K. Amano, M. Inoue, K. Hirano, S. Naito, H. Someya, I. Oowada, T. Kurashige, M. Shiki, S. Yoshimori, K. Yoshimura, and P. Davis, "Fast physical random bit generation with chaotic semiconductor lasers," *Nature Photon.*, vol. 2, pp. 728–732, Dec. 2008.

[2] F.Y. Lin and J.M. Liu, "Chaotic lidar," *IEEE Sel. Top. Quantum Electron.*, vol. 10, no. 5, pp. 991-997, Sep./Oct. 2004.

[3] Y. C. Wang, B. J. Wang, and A. B. Wang, "Chaotic correlation optical time domain reflectometer utilizing laser diode," *IEEE Photon. Technol. Lett.*, vol. 20, no. 19, pp. 1636–1638, Oct. 2008.

[4] V. Annovazzi-Lodi, S. Donati, and M. Manna, "Chaos and locking in a semiconductor laser due to external injection," *IEEE J. Quantum Electron.*, vol. 30, no. 7, pp. 1537–1541, Jul. 1994.

[5] H. F. Chen and J. M. Liu, "Open-loop chaotic synchronization of injection-locked semiconductor lasers with gigahertz range modulation," *IEEE J. Quantum Electron.*, vol. 36, no. 1, pp. 27-34, Jan. 2000.

[6] R. Vicente, C. R. Mirasso, and I. Fischer, "Simultaneous bidirectional message transmission in a chaos-based communication scheme," *Opt. Lett.*, vol. 32, pp. 403–405, Feb. 2007.

[7] S. K. Hwang, H. F. Chen, and C. Y. Lin, "All-optical frequency conversion using nonlinear dynamics of semiconductor lasers," *Opt. Lett.*, vol. 34, pp. 812–814, Mar. 2009.

[8] S. K. Hwang, S.C. Chan, S.C. Hsieh, and C.Y. Li, "Photonic microwave generation and transmission using direct modulation of stably injection-locked semiconductor lasers," *Opt. Commun.*, vol. 284, pp. 3581-3589, Jul. 2011.

[9] S. C. Chan, Q. Liu, Z. Wang, and K. S. Chiang, "Tunable negative-tap photonic microwave filter based on a cladding-mode coupler and an optically injected laser of large detuning," *Opt. Exp.*, vol. 19, pp. 12045–12052, Jun. 2011.

[10] S. C. Chan and J. M. Liu, "Tunable narrow-linewidth photonic microwave generation using semiconductor laser dynamics," *IEEE J. Sel. Topics Quantum Electron.*, vol. 10, no. 5, pp. 1025–1032, Sep./Oct. 2004.

[11] M. Pochet, N. A. Naderi, Y. Li, V. Kovanis, and L. F. Lester, "Tunable photonic oscillators using optically injected quantum-dash diode lasers," *IEEE Photon. Technol. Lett.*, vol. 22, no. 11, pp. 763–765, Jun. 2010.

[12] C. Cui, X. Fu, and S. C. Chan, "Double-locked semiconductor laser for radio-over-fiber uplink transmission," *Opt. Lett.*, vol. 34, no. 24, pp. 3821–3823, Dec. 2009.

[13] S. C. Chan, "Analysis of an optically injected semiconductor laser for microwave generation," *IEEE J. Quantum Electron.*, vol. 46, no. 3, pp. 421–428, Mar. 2010.

[14] C. Cui and S. C. Chan, "Performance analysis on using period-one oscillation of optically injected semiconductor lasers for radio-over-fiber uplinks," *IEEE J. Quantum Electron.*, vol. 48, pp. 490-499, Apr. 2012.

[15] J. P. Yao, "Microwave photonics," *IEEE J. Lightw. Technol.*, vol. 27, no. 3, pp. 314-335, Feb. 2009.

[16] R. Lang, "Injection locking properties of a semiconductor laser," *IEEE J. Quantum Electron.*, vol. 18, no. 6, pp. 976–983, Jun. 1982.

[17] S. C. Chan, S. K. Hwang, and J. M. Liu, "Period-one oscillation for photonic microwave transmission using an optically injected semiconductor laser", *Optics Express*, vol. 15, no. 22, pp. 14921-14935, Oct. 2007.